

Phonon-induced decoherence for a quantum dot spin qubit operated by Raman passage

K. Roszak,¹ A. Grodecka,¹ P. Machnikowski,^{1,2,*} and T. Kuhn²

¹*Institute of Physics, Wrocław University of Technology, 50-370 Wrocław, Poland*

²*Institut für Festkörpertheorie, Westfälische Wilhelms-Universität, 48149 Münster, Germany*

We study single-qubit gates performed via stimulated Raman adiabatic passage (STIRAP) on a spin qubit implemented in a quantum dot system in the presence of phonons. We analyze the interplay of various kinds of errors resulting from the carrier-phonon interaction as well as from quantum jumps related to nonadiabaticity and calculate the fidelity as a function of the pulse parameters. We give quantitative estimates for an InAs/GaAs system and identify the parameter values for which the error is considerably minimized, even to values below 10^{-4} per operation.

PACS numbers: 03.67.Lx, 03.65.Yz, 53.20.Kr, 42.50.Hz

I. INTRODUCTION

Quantum dots (QDs), among many other systems,¹ are considered to be promising candidates for an implementation of quantum information processing schemes. Due to their atomic-like structure² one can easily single out a subset of states to encode the logical qubit values. In principle, these systems provide for stable coherent memory if the information is encoded into the long-living electron spin,³ which motivated a spin-based proposal for quantum information storage and processing.⁴ On the other hand, experimental demonstrations of coherent control over the charge (orbital) degrees of freedom^{5,6,7,8,9} and the recently performed two-qubit gate based on a confined biexciton system¹⁰ prove the feasibility of quantum coherent manipulation of carrier states on picosecond time scales. It has been therefore proposed¹¹ to implement the qubit states as the vacuum and single exciton states in a QD, switched by resonant optical coupling and providing the two-qubit conditional gating via inter-QD dipole-dipole interaction.

Both the spin-based and the charge-based proposals suffer from serious difficulties. The spin switching time in typical structures is very long due to weak magnetic coupling. The orbital degrees of freedom do not provide for long operation times due to the finite exciton lifetime, usually of order of 1 ns.^{12,13} It seems therefore natural to seek for a scheme in which the logical values are stored using spin states, while the operations are performed via optical coupling to the charge degrees of freedom^{14,15}, also using QD systems in QED cavities.^{16,17} A promising solution, proposed recently,¹⁸ is to encode the qubit states into spin states of an excess electron in a QD and perform an arbitrary rotation¹⁹ by employing the stimulated Raman adiabatic passage (STIRAP) to a state localized spatially in a neighboring dot.²⁰ (An alternative scheme not relying on the auxiliary state has also been proposed²¹). Although this passage requires coupling to a charged exciton (X^- , or trion) state which has a finite lifetime, this state is never occupied (in the ideal case) so that the scheme is not affected by the decoherence resulting from its decay.

The essential difference between the atomic systems, where such quantum-optical schemes are successfully applied,²² and the solid state QD systems, where their new implementation is proposed, is the nature of the environment. In high-quality samples at low temperatures the dominant coupling to the external degrees of freedom is that involving lattice modes (phonons). The coupling mechanisms include interaction with lattice polarization (longitudinal optical, LO, phonons) and with piezoelectric fields induced by phonon-related strain (longitudinal and transverse acoustic, LA and TA, phonons) as well as the effective influence of strain-induced band shift, described in terms of the deformation potential coupling to LA phonons. Even restricted to acoustic phonons, this kind of external bath shows various peculiarities compared to models usually assumed in general studies.²³ Its low-frequency behavior depends on the coupling mechanism and on the wave-function geometry and is always super-ohmic, i.e., its spectral density grows super-linearly with frequency.²⁴ Due to the localization of carrier wave-functions on a scale much larger than the lattice constant, a high-frequency exponential cut-off in the effective phonon spectral densities appears. Moreover, apart from the nondiagonal coupling terms describing real transitions, there is usually a diagonal coupling which leads to pure dephasing effects^{24,25} resulting from the lattice relaxation after a fast (compared to phonon frequencies) change of the carrier state.^{25,26} Such an effect manifests itself in optical experiments as a fast partial decay of the signal coherence^{9,12} in excellent agreement with theoretical modeling assuming its phonon-related origin.²⁷

The characteristic time scales of these intrinsically non-Markovian pure dephasing processes are determined by the localization (QD size) and are typically much shorter than any real phonon-induced transition process. More importantly, they overlap with the time scales proposed for optical qubit control.¹¹ It has been shown²⁸ that the demand to avoid these pure dephasing effects limits from below the gating times, thus shrinking the time scale window defined, on the other side, by the long-time decoherence processes (e.g. the exciton lifetime).

In this paper we study the influence of the coupling to

the phonon degrees of freedom on the fidelity of the single qubit rotation via the STIRAP process¹⁹ implemented in the double-QD structure.¹⁸ Even if the possible phonon transitions to other states may be neglected, the diagonal terms still give rise not only to pure dephasing effects but also to transitions between the trapped carrier-field states. The probability of these phonon-induced transitions becomes very high if the spacing between the trapped energy levels falls into the area of high phonon spectral density and the overall error is roughly proportional to the process duration. We discuss how these strong decoherence processes may be avoided by either decreasing the trapped level separation (low-frequency regime, exploiting the super-ohmic behavior of spectral densities) or increasing it beyond the cut-off (high frequency regime). We show that in both cases one encounters a trade-off situation, due to the opposite requirements for phonon-induced jumps (short duration) and for the fundamental adiabaticity condition and pure dephasing (slow operation): In the low-frequency regime, avoiding phonon-induced transitions contradicts the condition for avoiding nonadiabatic jumps between the trapped states, which may be overcome only by considerably extending the process duration. In the high-frequency case, there is a competition between the pure dephasing and the phonon-induced transitions that is overcome by increasing the trapped state splitting, taking advantage of the particular structure of the phonon spectral density for a double dot structure.

The paper is organized as follows. In the next Section we present the model of the system. The Section III provides a brief description of the STIRAP qubit rotation procedure for completeness and necessary reference. The subsequent Section IV contains the general derivation of the phonon-induced error for an arbitrary system evolution. The results of this section are applied to the STIRAP procedure in the central Section V, where some general discussion is also contained. In the Section VI we present the results for specific pulse shapes in order to get some quantitative estimates. Finally, the Section VII summarizes and concludes the paper. In addition, some technical details and further analysis are presented in the Appendices.

II. THE MODEL

The Hamiltonian describing this system and its coupling to lattice modes may be written as

$$H = H_C + H_{\text{ph}} + V, \quad (1)$$

The first term is the STIRAP Hamiltonian including both the qubit states and the control fields. The implementation¹⁸ defines the qubit by two spin states of a single excess electron in one of the QDs (“large”) from a vertically stacked pair. In order to perform a general single-qubit rotation between the two qubit states $|0\rangle$ and $|1\rangle$ an auxiliary state $|2\rangle$ is used¹⁹, in which the electron

is shifted to the second (“small”) dot and has the same spin orientation as in $|0\rangle$. All these three states are coupled to a fourth state $|3\rangle$, a charged exciton (trion) state, by laser beams $\Omega_0, \Omega_1, \Omega_2$. The Hamiltonian for such a system in rotating wave approximation (RWA) is

$$H_C = \sum_n \epsilon_n |n\rangle\langle n| + \sum_{n=0}^2 \Omega_n(t) \left(e^{i(\omega_n t - \delta_n)} |n\rangle\langle 3| + \text{H.c.} \right), \quad (2)$$

where the slowly varying pulse envelopes $\Omega_n(t)$ are real and positive, ω_n are the corresponding laser frequencies and δ_n are the phases.

The second term describes the free phonon evolution,

$$H_{\text{ph}} = \sum_{\mathbf{k}} \hbar \omega_{\mathbf{k}} \beta_{\mathbf{k}}^\dagger \beta_{\mathbf{k}},$$

where $\beta_{\mathbf{k}}^\dagger, \beta_{\mathbf{k}}$ are phonon creation and annihilation operators (with respect to the crystal ground state). Throughout the paper, the phonon branch index will be implicit in \mathbf{k} , unless it is explicitly written.

The final term is the carrier-phonon interaction. Since the adiabaticity inherent in the STIRAP procedure excludes the possibility of inducing high-frequency dynamics and also all the trapped state splittings should be at most of several meV (to avoid crossing with excited carrier states), the discussion will be restricted to acoustic phonons. The corresponding Hamiltonian is

$$V = \sum_{n,n'=0}^3 |n\rangle\langle n'| f_{nn'}(\mathbf{k}) \left(\beta_{\mathbf{k}} + \beta_{-\mathbf{k}}^\dagger \right). \quad (3)$$

The coupling constants include all the coupling mechanisms relevant for a given phonon branch and have the symmetry $f_{nn'}(\mathbf{k}) = f_{n'n}^*(-\mathbf{k})$. If both states n, n' are single-electron states, then^{29,30}

$$f_{nn'}^{(l)}(\mathbf{k}) = \sqrt{\frac{\hbar}{2\rho V \omega_l(\mathbf{k})}} \left[\sigma k - i \frac{de}{\varepsilon_0 \varepsilon_1} M_l(\hat{\mathbf{k}}) \right] \mathcal{F}_{nn'}(\mathbf{k}), \quad (4a)$$

and

$$f_{nn'}^{(t_1, t_2)}(\mathbf{k}) = -i \sqrt{\frac{\hbar}{2\rho V \omega_t(\mathbf{k})}} \frac{de}{\varepsilon_0 \varepsilon_1} M_{t_1, t_2}(\hat{\mathbf{k}}) \mathcal{F}_{nn'}(\mathbf{k}), \quad (4b)$$

where l, t_1, t_2 refer to the longitudinal and two transverse acoustic phonon branches. Here e denotes the electron charge, ρ is the crystal density, V is the system volume, $\omega_{l,t}$ are the phonon frequencies, d is the piezoelectric constant, ε_0 is the vacuum dielectric constant, ε_1 is the static relative dielectric constant and σ is the deformation potential constant for electrons. The functions M_s depend

on the orientation of the phonon wavevector.³⁰ For the zinc-blende structure they are given by

$$M_s(\hat{\mathbf{k}}) = 2 \left[\hat{k}_x \hat{k}_y (\hat{e}_{s,\mathbf{k}})_z + \hat{k}_y \hat{k}_z (\hat{e}_{s,\mathbf{k}})_x + \hat{k}_z \hat{k}_x (\hat{e}_{s,\mathbf{k}})_y \right],$$

where $\hat{\mathbf{k}} = \mathbf{k}/k$ and $\hat{e}_{s,\mathbf{k}}$ is the unit polarization vector for the wavevector \mathbf{k} and polarization s . Finally, the form-factors $\mathcal{F}_{nn'}(\mathbf{k})$ depend on the wave-function geometry and, for single-electron states, are given by

$$\mathcal{F}_{nn'}(\mathbf{k}) = \int d^3\mathbf{r} \Psi_n^*(\mathbf{r}) e^{i\mathbf{k}\cdot\mathbf{r}} \Psi_{n'}(\mathbf{r}), \quad (5)$$

where $\Psi_n(\mathbf{r})$ is the envelope wave-function of the electron.

We will assume that the two spin states used to encode $|0\rangle$ and $|1\rangle$ correspond to the same orbital wave-functions so that the couplings $f_{00}(\mathbf{k})$ and $f_{11}(\mathbf{k})$ are equal. The couplings $f_{01}(\mathbf{k})$, $f_{10}(\mathbf{k})$, $f_{12}(\mathbf{k})$ and $f_{21}(\mathbf{k})$ vanish since the spin orientation in the state $|1\rangle$ differs from that in $|0\rangle$ and $|2\rangle$ (spin-orbit coupling that might lead to phonon-assisted spin flip is very weak for electrons). Moreover, it is assumed that there is no overlap of wave-functions between the states $|0\rangle$ and $|2\rangle$, so that also $f_{02}(\mathbf{k})$ and $f_{20}(\mathbf{k})$ vanish.

An important point is that, since the electron resides normally in the large dot, at the initial moment the lattice is relaxed to the corresponding minimum (“dressing” of the electron in the coherent deformation field). This may be accounted for by defining the modes with respect to this shifted equilibrium, so that the ground state of the interacting system corresponds to the new phonon vacuum, i.e., by transforming to new phonon operators b_n according to

$$b_{\mathbf{k}} = \beta_{\mathbf{k}} + \frac{f_{00}^*(\mathbf{k})}{\omega_{\mathbf{k}}}.$$

Upon transformation to these new modes the interaction (3) reads

$$V = \sum_{n=2,3} |n\rangle\langle n| \sum_{\mathbf{k}} F_{nn}(\mathbf{k}) (b_{\mathbf{k}} + b_{-\mathbf{k}}^\dagger) + \left[\sum_{n=0}^2 |n\rangle\langle 3| \sum_{\mathbf{k}} f_{n3}(\mathbf{k}) (b_{\mathbf{k}} + b_{-\mathbf{k}}^\dagger) + \text{H.c.} \right],$$

where $F_{nn}(\mathbf{k}) = f_{nn}(\mathbf{k}) - f_{00}(\mathbf{k})$. Moreover, the carrier Hamiltonian undergoes a renormalization which is, however, inessential for our discussion. In the rotating frame, defined by $|\tilde{n}\rangle = e^{-i(\omega_n t - \tilde{\delta}_n)} |n\rangle$, $\tilde{\delta}_n = \delta_n - \delta_0$, $n = 0, 1, 2$, the interaction Hamiltonian reads

$$V = \sum_{n=2,3} |\tilde{n}\rangle\langle \tilde{n}| \sum_{\mathbf{k}} F_{nn}(\mathbf{k}) (b_{\mathbf{k}} + b_{-\mathbf{k}}^\dagger) + \left[\sum_{n=0}^2 |\tilde{n}\rangle\langle 3| \sum_{\mathbf{k}} F_{n3}(\mathbf{k}) (b_{\mathbf{k}} + b_{-\mathbf{k}}^\dagger) + \text{H.c.} \right]. \quad (6)$$

where $F_{n3}(\mathbf{k}) = f_{n3}(\mathbf{k}) e^{i(\omega_n t - \tilde{\delta}_n)}$. It is clear from Eq. (6) that the phonons influence the dynamics only when a transfer from the large dot to a spatially different carrier state (small dot or trion state) occurs.

III. THE STIRAP PROCEDURE FOR A SINGLE-QUBIT ROTATION

In order to achieve the Raman coupling, the detunings from the corresponding dipole transition energies must be the same for all the three laser frequencies. Therefore, we put $\omega_n = \epsilon_3 - \epsilon_n - \Delta$, $n = 0, 1, 2$. The RWA Hamiltonian (2) may now be written

$$H_C = \Delta |3\rangle\langle 3| + \frac{1}{2} \sum_{n=0}^2 \Omega_n(t) (e^{i\tilde{\delta}_n} |\tilde{n}\rangle\langle 3| + e^{-i\tilde{\delta}_n} |3\rangle\langle \tilde{n}|).$$

The envelopes of the first two pulses are proportional to each other,

$$\Omega_0(t) = \Omega_{01}(t) \cos \chi, \quad \Omega_1(t) = \Omega_{01}(t) \sin \chi, \quad \chi \in (0, \frac{\pi}{2}).$$

In terms of the rotated basis states

$$\begin{aligned} |B\rangle &= \cos \chi |\tilde{0}\rangle + e^{i\tilde{\delta}_1} \sin \chi |\tilde{1}\rangle, \\ |D\rangle &= -\sin \chi |\tilde{0}\rangle + e^{i\tilde{\delta}_1} \cos \chi |\tilde{1}\rangle, \end{aligned}$$

the Hamiltonian now reads

$$H_C = \Delta |3\rangle\langle 3| + \frac{1}{2} \Omega_{01}(t) (|B\rangle\langle 3| + |3\rangle\langle B|) + \frac{1}{2} \Omega_2(t) (e^{i\tilde{\delta}_2} |\tilde{2}\rangle\langle 3| + e^{-i\tilde{\delta}_2} |3\rangle\langle \tilde{2}|). \quad (7)$$

Hence, the pulses affect only one linear combination of the qubit states, the coupled (bright) state $|B\rangle$, while the other orthogonal combination, $|D\rangle$, remains unaffected. At a fixed time t , the Hamiltonian (7) has the eigenstates

$$|a_0\rangle = \cos \theta |B\rangle - e^{i\tilde{\delta}_2} \sin \theta |\tilde{2}\rangle \quad (8a)$$

$$|a_-\rangle = \cos \phi (\sin \theta |B\rangle + e^{i\tilde{\delta}_2} \cos \theta |\tilde{2}\rangle) - \sin \phi |3\rangle, \quad (8b)$$

$$|a_+\rangle = \sin \phi (\sin \theta |B\rangle + e^{i\tilde{\delta}_2} \cos \theta |\tilde{2}\rangle) + \cos \phi |3\rangle, \quad (8c)$$

where

$$\tan \theta = \frac{\Omega}{\Omega_2}, \quad \sin \phi = \frac{1}{\sqrt{2}} \left(1 - \frac{\Delta}{\sqrt{\Delta^2 + \Omega^2 + \Omega_2^2}} \right)^{1/2}.$$

The corresponding eigenvalues are

$$\lambda_0 = 0, \quad \lambda_{\pm} = \frac{\Delta \pm \sqrt{\Delta^2 + \Omega^2 + \Omega_2^2}}{2}. \quad (9)$$

The system evolution is realized by an adiabatic change of the pulse amplitudes (see Fig. 1; in this application, the detuning remains constant). Initially (at the time

t_0), both pulses are switched off, hence $\phi = 0$, then Ω_2 is switched on first, hence also $\theta = 0$. Therefore, $|a_0\rangle$ coincides with $|B\rangle$ and $|a_-\rangle$ with $|2\rangle$. During an adia-

batic evolution of the parameters, the states move along the corresponding spectral branches, and the evolution operator may be written (in the basis $|B\rangle, |\tilde{2}\rangle, |3\rangle$)

$$U_C(t) = \begin{pmatrix} \cos \theta & e^{-i\Lambda_-} \cos \phi \sin \theta & e^{-i\Lambda_+} \sin \phi \sin \theta \\ -e^{i\tilde{\delta}_2} \sin \theta & e^{i(\tilde{\delta}_2 - \Lambda_-)} \cos \phi \cos \theta & e^{i(\tilde{\delta}_2 - \Lambda_+)} \sin \phi \cos \theta \\ 0 & -e^{-i\Lambda_-} \sin \phi & e^{-i\Lambda_+} \cos \phi \end{pmatrix}, \quad (10)$$

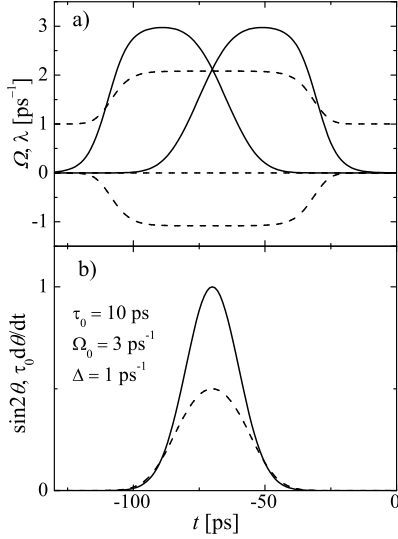


FIG. 1: (a) An example of pulse shapes (solid) and the resulting structure of the dresses levels (dashed). (b) The evolution of the functions $\dot{\theta}$ (dashed) and $\sin 2\theta$ (solid) for the pulse sequence shown in (a).

where $\theta, \phi, \lambda_{\pm}$ and $\tilde{\delta}_2$ are slowly varying functions of time and

$$\Lambda_{\pm}(t) = \int_0^t d\tau \lambda_{\pm}(\tau).$$

As shown in Ref. 19, performing the transfer from $\theta = 0$ to $\theta = \pi/2$ and then back with a different phase $\tilde{\delta}_2$ of the Ω_2 pulse results in a rotation in the qubit space $|0\rangle, |1\rangle$ around the axis determined by χ and by the relative phase $\tilde{\delta}_1$ between Ω_0 and Ω_1 . The rotation angle is equal to the difference of the $\tilde{\delta}_3$ phases in the first and second pulse sequence. Ideally, the state $|2\rangle$ is only occupied during gating, while the state $|3\rangle$ is never occupied.

The above procedure works under the assumption that the evolution is perfectly adiabatic. However, any change of parameters can never be infinitely slow and the probability of a jump from $|a_0\rangle$ to one of the two other states $|a_{\pm}\rangle$ remains finite. In the lowest order, the correspond-

ing probability amplitudes are³¹

$$c_{\pm}(t) = \int_{t_0}^t d\tau \langle a_{\pm}(t) | \psi(t) \rangle \exp \left[-i \int_{\tau}^t \lambda_{\pm}(\tau') d\tau' \right],$$

where $\psi(t)$ is the state evolving adiabatically from the initial one. Let us write the general initial state in the form

$$|\psi_0\rangle = \cos \frac{\vartheta}{2} |B\rangle - e^{i\varphi} \sin \frac{\vartheta}{2} |D\rangle. \quad (11)$$

The qubit rotation¹⁹ is performed by two well separated, mirror-symmetric pulse sequences differing only by a phase. Thus, using the explicit formulas (8a-c) one may write

$$c_{\pm}(t) = \cos \frac{\vartheta}{2} e^{-i\Lambda_{\pm}(t)} [\tilde{c}_{\pm} - \tilde{c}_{\pm}^*], \quad (12)$$

where

$$\tilde{c}_{\pm} = \int_{-\infty}^{\infty} d\tau \left[\frac{\sin \phi(\tau)}{\cos \phi(\tau)} \right] \dot{\theta}(\tau) e^{i\Lambda_{\pm}(\tau)}, \quad (13)$$

with $\sin \phi(\tau)$, $\cos \phi(\tau)$ corresponding to ‘+’ and ‘-’, respectively, and the integral involves only one pulse sequence. If the evolution induced by the pulse sequence is symmetric with respect to a certain time t_1 the amplitude (13) may be written in the form $\tilde{c}_{\pm} = ie^{i\Lambda_{\pm}(t_1)} |\tilde{c}_{\pm}|$.

In order to discuss the general properties of the nonadiabatic jump amplitudes, let us write the evolution of θ in the form

$$\theta(t) = \tilde{\theta} \left(\frac{t - t_1}{\tau_0} \right), \quad (14)$$

where $\tilde{\theta}$ is a function of unit width, so that τ_0 is the time scale of the evolution of θ . (The total duration of the gate, including two pulse sequences, is roughly an order of magnitude longer). If the functions $\phi(t)$ and $\lambda_{\pm}(t)$ change slowly around $t = t_1$, then

$$|\tilde{c}_{\pm}| \approx \left[\frac{\sin \phi(t_1)}{\cos \phi(t_1)} \right] g_0[\tau_0 \lambda_{\pm}(t_1)],$$

where

$$g_0(x) = \int du \tilde{\theta}'(u) e^{iux}$$

is a function of unit width, with a fixed value at $x = 0$ and vanishing for $x \gg 1$. Hence, the nonadiabatic jump amplitudes (12) are small when

$$\lambda_{\pm} \gg 1/\tau_0, \quad (15)$$

which is the standard adiabaticity condition.

It is interesting to note that for symmetric pulses the final transition probabilities (12) vanish for $\Lambda_{\pm}(t_1) = (n + 1/2)\pi$. This fact is due to destructive interference of the jump amplitudes during the first and the second pulse sequence. Although it might be tempting to exploit this cancellation and perform a successful passage for times and laser beam parameters that do not satisfy the condition (15), such a procedure requires a detailed knowledge of the excitonic dipole moments and a precise control over the laser beam properties. Moreover, the cancellation takes place only in the final state, while during the process the other states are occupied, which leads to the nonvanishing occupation of the X^- state and to decoherence, contrary to the original motivation of this qubit implementation. In order to avoid these effects, the envelopes of the transition probabilities should be used as the actual bound to the nonadiabatic-jump-related error.

IV. PHONON-INDUCED DECOHERENCE: GENERAL THEORY

In this section we derive the equations for the reduced density matrix of the carrier subsystem in the leading order in the phonon coupling, assuming that the unperturbed (ideal) evolution of the noninteracting system, described by the unitary evolution operator

$$U_0(t) = U_C(t) \otimes e^{-iH_{\text{ph}}t}$$

is known (see also Ref. 32).

The interaction between the carriers and the phonon modes [Eq. (6)] has the general form

$$V = \sum_{nn'} S_{nn'} \otimes R_{nn'}, \quad (16)$$

where $S_{nn'} = S_{n'n}^{\dagger} = |n\rangle\langle n'|$ (n, n' run over the states $|B\rangle, |\tilde{2}\rangle, |3\rangle$) act in the Hilbert space of the carrier subsystem and

$$R_{nn'} = R_{n'n}^{\dagger} = \sum_{\mathbf{k}} F_{nn'}(\mathbf{k}) (b_{\mathbf{k}} + b_{-\mathbf{k}}^{\dagger}), \quad (17)$$

with $F_{nn'}(\mathbf{k}) = F_{n'n}^*(-\mathbf{k})$, affect only the phonon environment.

We assume that at the initial time t_0 the system is in the product state

$$\varrho(t_0) = \rho_0 \otimes \rho_T, \quad \rho_0 = |\psi_0\rangle\langle\psi_0|, \quad (18)$$

where $|\psi_0\rangle$ is a certain state of the carrier subsystem and ρ_T is the thermal equilibrium distribution of phonon

modes. Physically, this is justified by the existence of two distinct time scales: the long one for the carrier decoherence (e.g. about 1 ns ground state exciton lifetime^{12,13}) and the short one for the reservoir relaxation (1 ps pure dephasing time^{12,24,26}).

The starting point is the evolution equation for the density matrix of the total system in the interaction picture with respect to the externally driven evolution U_0 , in the second order Born approximation with respect to the carrier-phonon interaction³³

$$\begin{aligned} \tilde{\varrho}(t) = & \tilde{\varrho}(t_0) + \frac{1}{i\hbar} \int_{t_0}^t d\tau [V(\tau), \varrho(t_0)] \\ & - \frac{1}{\hbar^2} \int_{t_0}^t d\tau \int_{t_0}^{\tau} d\tau' [V(\tau), [V(\tau'), \varrho(t_0)]], \end{aligned} \quad (19)$$

where

$$\tilde{\varrho}(t) = U_0^{\dagger}(t) \varrho(t) U_0(t), \quad V(t) = U_0^{\dagger}(t) V U_0(t).$$

The reduced density matrix of the carrier subsystem is

$$\rho(t) = U_C(t) [\text{Tr}_R \tilde{\varrho}(t)] U_C^{\dagger}(t),$$

where the trace is taken over the reservoir degrees of freedom. The first (zeroth order) term in (19) obviously yields

$$\rho^{(0)}(t) = U_C(t) |\psi_0\rangle\langle\psi_0| U_C^{\dagger}(t) = |\psi_0(t)\rangle\langle\psi_0(t)|. \quad (20)$$

The second term vanishes, since it contains the thermal average of an odd number of phonon operators. The third (second order) term describes the leading phonon correction to the dynamics of the carrier subsystem,

$$\begin{aligned} \tilde{\rho}^{(2)}(t) = & \\ & - \frac{1}{\hbar^2} \int_{t_0}^t d\tau \int_{t_0}^{\tau} d\tau' \text{Tr}_R [V(\tau), [V(\tau'), \varrho(t_0)]]. \end{aligned} \quad (21)$$

The first of the four terms resulting from expanding the commutators in (21) is $-Q_t \rho_0$, where

$$\begin{aligned} Q_t = & \frac{1}{\hbar^2} \sum_{nn'} \sum_{mm'} \int_{t_0}^t d\tau \int_{t_0}^{\tau} d\tau' \\ & \times S_{nn'}(\tau) S_{mm'}(\tau') \langle R_{nn'}(\tau - \tau') R_{mm'} \rangle. \end{aligned}$$

The operators S and R are transformed into the interaction picture in the usual way

$$S_{nn'}(t) = U_0^{\dagger}(t) S_{nn'} U_0(t), \quad R_{nn'}(t) = U_0^{\dagger}(t) R_{nn'} U_0(t)$$

and $\langle \hat{O} \rangle = \text{Tr}_R [\hat{O} \rho_T]$ denotes the thermal average (obviously $[U_0(t), \rho_T] = 0$). Using the symmetry of the operators $S_{nn'}$ and $R_{nn'}$ the second term may be written as $-\rho_0 Q_t^{\dagger}$. In a similar manner, the two other terms may be combined to $\hat{\Phi}_t[\rho_0]$, where

$$\begin{aligned} \hat{\Phi}_t[\rho] = & \frac{1}{\hbar^2} \sum_{nn'} \sum_{mm'} \int_{t_0}^t d\tau \int_{t_0}^{\tau} d\tau' \\ & \times S_{nn'}(\tau') \rho S_{mm'}(\tau) \langle R_{mm'}(\tau - \tau') R_{nn'} \rangle. \end{aligned}$$

In terms of the new hermitian operators

$$A_t = Q_t + Q_t^\dagger, \quad h_t = \frac{1}{2i}(Q_t - Q_t^\dagger), \quad (22)$$

the perturbation to the density matrix at the final time t (21) may be written as

$$\rho^{(2)}(t) = -i[h_t, \rho_0] - \frac{1}{2}\{A_t, \rho_0\} + \hat{\Phi}_t[\rho_0]. \quad (23)$$

The first term is a Hamiltonian correction which does not lead to irreversible effects and in principle may be compensated for by an appropriate modification of the control Hamiltonian H_C . The other two terms describe processes of entangling the system with the reservoir, leading to the loss of coherence of the carrier state.

Introducing the spectral density of the reservoir,

$$\begin{aligned} R_{nn',mm'}(\omega) &= \frac{1}{2\pi\hbar^2} \int dt \langle R_{nn'}(t) R_{mm'} \rangle e^{i\omega t} \\ &= \frac{1}{\hbar^2} \sum_{\mathbf{k}} F_{nn'}(\mathbf{k}) F_{m'm}^*(\mathbf{k}) \\ &\quad \times [(n_{\mathbf{k}} + 1)\delta(\omega - \omega_{\mathbf{k}}) + n_{\mathbf{k}}\delta(\omega + \omega_{\mathbf{k}})], \end{aligned} \quad (24)$$

[using the explicit form (17); $n_{\mathbf{k}}$ are phonon occupation

numbers] one may write

$$\hat{\Phi}_t[\rho] = \sum_{nn'} \sum_{mm'} \int d\omega R_{nn',mm'}(\omega) Y_{mm'}(\omega) \rho Y_{n'n}^\dagger(\omega) \quad (25)$$

where the frequency-dependent operators have been introduced,

$$Y_{nn'}(\omega) = \int_{t_0}^t S_{nn'}(\tau) e^{i\omega\tau} d\tau. \quad (26)$$

Using (24) one has also

$$\begin{aligned} Q_t &= \sum_{nn'} \sum_{mm'} \int d\omega \int_{t_0}^t d\tau \int_{t_0}^t d\tau' \Theta(\tau - \tau') \\ &\quad \times S_{nn'}(\tau) S_{mm'}(\tau') R_{nn',mm'}(\omega) e^{-i\omega(\tau - \tau')}. \end{aligned}$$

Next, representing the Heaviside function as

$$\Theta(t) = -e^{i\omega t} \int \frac{d\omega'}{2\pi i} \frac{e^{-i\omega' t}}{\omega' - \omega + i0^+},$$

we write

$$\begin{aligned} Q_t &= - \sum_{nn'} \sum_{mm'} \int d\omega R_{nn',mm'}(\omega) \int \frac{d\omega'}{2\pi i} \frac{Y_{n'n}^\dagger(\omega') Y_{mm'}(\omega')}{\omega' - \omega + i0^+} \\ &= - \sum_{nn'} \sum_{mm'} \int d\omega R_{nn',mm'}(\omega) \int \frac{d\omega'}{2\pi i} Y_{n'n}^\dagger(\omega') Y_{mm'}(\omega') \left[-i\pi\delta(\omega' - \omega) + \mathcal{P} \frac{1}{\omega' - \omega} \right], \end{aligned}$$

where \mathcal{P} denotes the principal value.

Hence, the two Hermitian operators defined in (22) take the form

$$A_t = \sum_{nn'} \sum_{mm'} \int d\omega R_{nn',mm'}(\omega) Y_{n'n}^\dagger(\omega) Y_{mm'}(\omega) \quad (27)$$

and

$$\begin{aligned} h_t &= \\ &\sum_{nn'} \sum_{mm'} \int d\omega R_{nn',mm'}(\omega) \mathcal{P} \int \frac{d\omega'}{2\pi} \frac{Y_{n'n}^\dagger(\omega') Y_{mm'}(\omega')}{\omega' - \omega}. \end{aligned} \quad (28)$$

In the quantum information processing context it is customary to quantify the quality of the operation in terms of the fidelity, which is a measure of the overlap between the desired (unperturbed) state and the actual final state, $F = \text{Tr}[U_C(t, t_0) \rho_0 U_C^\dagger(t, t_0) \rho(t)]$. The error is then defined as the fidelity loss, $\delta = 1 - F$. From Eqs.

(20) and (23) one has

$$\begin{aligned} \delta &= -\langle \psi_0 | \hat{\rho}^{(2)} | \psi_0 \rangle \\ &= \sum_{nn',mm'} \int d\omega R_{nn',mm'}(\omega) \\ &\quad \times \langle \psi_0 | Y_{n'n}^\dagger(\omega) \mathbf{P}^\perp Y_{mm'}(\omega) | \psi_0 \rangle, \end{aligned} \quad (29)$$

where \mathbf{P}^\perp is the projector on the orthogonal complement of $|\psi_0\rangle$ in the carrier space. In this order the unitary correction generated by h_t does not contribute to the error.

V. INTERACTION WITH THE PHONON BATH DURING THE STIRAP PROCESS IN A QD SYSTEM

In this section we apply the general theory from Section IV to the qubit rotation performed via a STIRAP process, as described in Section III, implemented in the double-QD system.

The only nonvanishing nondiagonal coupling in the Hamiltonian (6) is $F_{n3}(\mathbf{k})$. Let us note, however, that for this coupling one has, according to (26),

$$Y_{n3}(\omega) = \sum_{mm'} \int dt e^{i[(\omega+\omega_n)t-\tilde{\delta}_n]} U_{Cnm}^* U_{C3m'} |\tilde{m}\rangle \langle \tilde{m}'|,$$

where U_{Cnm} are the elements of the evolution operator (10), varying at most with frequencies $\sim \lambda_{\pm}$. It is therefore clear that this function is peaked around $\omega \approx -\omega_n$, i.e. at the optical frequencies which are many orders of magnitude higher than any phonon frequencies present in $R_{nn',mm'}(\omega)$ [Eq. (24)]. Thus, inter-band nondiagonal phonon couplings do not contribute to (29). This is consistent with the rotating wave approximation and may also be understood by noting that the second Born approximation accounts for processes that may be represented as a series of emission and absorption processes involving arbitrarily many photons but only one phonon. Each photon process takes the system from the states 0, 1, 2 to 3 with the exchange of a large energy while a nondiagonal phonon process produces the same state change but with negligible energy exchange. Thus, energy can never be conserved in a process involving the inter-band phonon term.

Since the adiabatic evolution U_C does not transfer qubit states into $|3\rangle$, $U_C^\dagger|3\rangle$ remains orthogonal to $|B\rangle$. Hence, $Y_{33}(\omega)$ does not contribute to (29) and we may write

$$\delta = \int d\omega \frac{R(\omega)}{\omega^2} S(\omega), \quad R(\omega) \equiv R_{22,22}(\omega), \quad (30)$$

with

$$S(\omega) = \omega^2 \sum_n |\langle \psi_0 | Y_2^\dagger(\omega) | \psi_n \rangle|^2 = \sum_n |s_n(\omega)|^2, \quad (31)$$

where the sum runs over a complete set of states $|\psi_n\rangle$ orthogonal to $|\psi_0\rangle$.

For the initial state (11), using the explicit evolution operator (10), the contributions from the three states $|\psi_n\rangle = \sin \frac{1}{2} \vartheta |B\rangle + e^{i\varphi} \cos \frac{1}{2} \vartheta |D\rangle, |2\rangle, |3\rangle$ are, respectively,

$$s_1(\omega) = -\frac{\omega}{2} \sin \vartheta \int_{-\infty}^{\infty} dt e^{-i\omega t} \sin^2 \theta(t), \quad (32)$$

$$s_{2,3}(\omega) = -\frac{\omega}{2} \cos \frac{\vartheta}{2} \int_{-\infty}^{\infty} dt e^{-i\omega t} \begin{bmatrix} \cos \phi(t) \\ \sin \phi(t) \end{bmatrix} \sin 2\theta(t) e^{-i\Lambda_{\mp}(t)}. \quad (33)$$

Following the argument that led to Eq. (12), these functions may be written in the form

$$s_n(\omega) = 2u_n(\vartheta) \text{Re}[\tilde{s}_i(\omega)],$$

where $u_1 = \frac{1}{2} \sin \vartheta$, $u_{2,3} = \cos(\vartheta/2)$, and

$$\begin{aligned} \tilde{s}_1(\omega) &= i \int dt e^{-i\omega t} \sin 2\theta(t) \dot{\theta}(t) \\ &= e^{-i\omega t_1} |\tilde{s}_1(\omega)|, \end{aligned} \quad (34a)$$

$$\begin{aligned} \tilde{s}_{2,3}(\omega) &= -\frac{\omega}{2} \int dt e^{-i[\omega t + \Lambda_{\mp}(t)]} \begin{bmatrix} \cos \phi(t) \\ \sin \phi(t) \end{bmatrix} \sin 2\theta(t) \\ &= e^{-i(\omega t_1 + \Lambda_{\mp}(t_1))} |\tilde{s}_{2,3}(\omega)| \end{aligned} \quad (34b)$$

where the integrals are now over one pulse sequence and the final equalities hold for symmetric pulse sequences.

Using the representation (14) of the system evolution and denoting the Fourier transform of $\tilde{\theta}' \sin 2\tilde{\theta}$ by $g_1(x)$ we find $|\tilde{s}_1(\omega)| = g_1(\omega\tau_0)$. Since $t_1 \gg \tau_0$ and $|s_1(\omega)|^2$ is integrated with the slowly varying spectral density, the oscillating terms do not contribute and one may write

$$|s_1(\omega)|^2 \approx \frac{1}{2} \sin^2 \vartheta |g_1(\omega\tau_0)|^2.$$

Hence, the function, $s_1(\omega)$ is concentrated at $\omega = 0$ and broadened by a factor $1/\tau_0$ due to the time-dependence. It is responsible for the pure dephasing effect.²⁸ The resulting error, according to (30), will grow with broadening of $s_1(\omega)$ i.e. with decreasing process duration. Hence, similarly to the fundamental condition (15), it always favors slow operation. However, it is independent of the trapped level splittings and reflects only the low-frequency properties of the spectral density (at a given temperature). For $R(\omega) \approx R_0 \omega^n$, $n \geq 3$ this pure dephasing error at the temperature T is

$$\delta^{(\text{pd})} \sim \begin{cases} R_0 \tau_0^{-(n-1)}, & k_B T \ll \hbar/\tau_0 \\ R_0 \frac{k_B T}{\hbar} \tau_0^{-(n-2)}, & k_B T \gg \hbar/\tau_0. \end{cases} \quad (35)$$

It should be noted that for durations of the order of 10 ps the crossover from the low to high temperature behavior takes place at $T \sim 0.1$ K.

By a similar argument, the two other functions may be approximately written as

$$|s_{2,3}(\omega)|^2 \approx \frac{(\omega\tau_0)^2}{2} \cos^2 \frac{\vartheta}{2} \begin{bmatrix} \cos^2 \phi \\ \sin^2 \phi \end{bmatrix} g_2^2[(\omega + \lambda_{\mp})\tau_0],$$

where $g_2(x)$ is the Fourier transform of $\sin 2\tilde{\theta}(u)$. These functions have a similar $1/\tau_0$ broadening but are also shifted to the spectral position $\omega = -\lambda_{\pm}$. They describe the error resulting from phonon-assisted transitions between the trapped states $|a_{0,\pm}\rangle$ (see Appendix B for further support to this interpretation). In view of the condition (15), this shift must be larger than the broadening and for rough estimates the latter may be neglected (if the spectral density varies slowly on the scale of this broadening; the role of oscillations in the spectral density is discussed below). Hence, one may write $\delta^{(\text{tr})} = \delta_+^{(\text{tr})} + \delta_-^{(\text{tr})}$, where

$$\begin{aligned} \delta_{\mp}^{(\text{tr})} &= \int d\omega \frac{R(\omega)}{\omega^2} |s_{2,3}(\omega)|^2 \\ &\approx R(-\lambda_{\mp}) \int d\omega \left| \frac{s_{2,3}(\omega)}{\omega} \right|^2. \end{aligned} \quad (36)$$

The error is therefore proportional to

$$\delta \sim R(\lambda_{\pm}) \tau_0. \quad (37)$$

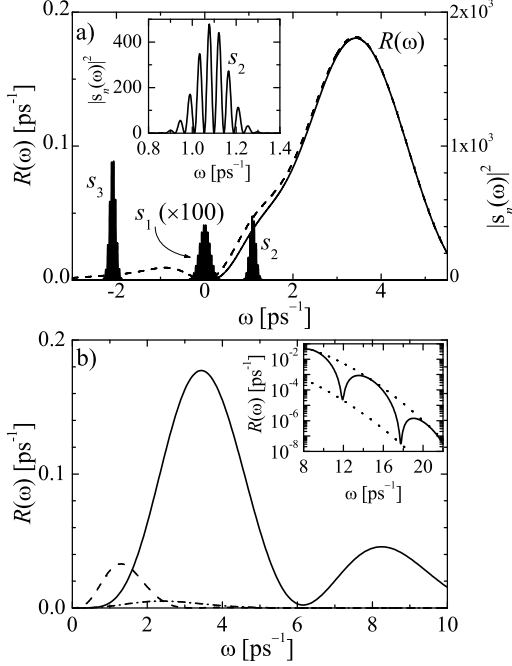


FIG. 2: (a) The functions $|s_n(\omega)|^2$ describing the phonon-induced errors (for pulses as in Fig. 1) and the total spectral density of the phonon reservoir $R(\omega)$ at $T = 0$ (solid) and $T = 5$ K (dashed) for the model InAs/GaAs system (Tab. I). The inset shows the exact shape of one of the spectral features. (b) The contributions to the spectral density at $T=0$: DP coupling to LA phonons (solid) and piezoelectric coupling to TA (dashed) and LA (dash-dotted) phonons. Inset: high-frequency behavior with the two bounds defined in Appendix A.

Thus, for a fixed spectrum of the trapped states this error grows linearly in time (in the leading order), which is a usual characteristics of real transition processes.

In order to maximize the fidelity of the coherent operation, one must find the trade-off between the errors caused by phonon-assisted transitions (37), which favors short process durations, and the other two restrictions, related to pure dephasing (35) and to the general adiabaticity condition (15) both increasing for fast evolution. As can be seen from the orders of magnitude of the spectral characteristics determining the error [Fig. 2 and Eq. (30)], in general, the fidelity may be strongly decreased. However, contrary to the simple excitonic qubit case²⁸, the STIRAP procedure in a QD system provides two ways to avoid this limitations.

First, due to the super-ohmic properties of the phonon spectral density, $R(\omega) \sim \omega^n$, $n \geq 2$, all error contributions may in principle be minimized by locating the trapped levels λ_{\pm} in the low-frequency sector and decreasing them while simultaneously increasing the gate duration τ_0 .

Second, the values of λ_{\pm} may be chosen sufficiently far beyond the cut-off frequency. The contribution from the

Static dielectric constant	ϵ_s	13.2
Piezoelectric constant	d	0.16 C/m ²
Longitudinal sound speed	c_l	5600 m/s
Transversal sound speed	c_t	2800 m/s
Deformation potential for electrons	σ	-8.0 eV
Density	ϱ	5360 kg/m ³
Electron wave-function widths:		
in-plane	l_{\perp}	5.0 nm
z-direction	l_z	1.5 nm
Dot separation	D	6.0 nm

TABLE I: The GaAs material parameters and QD system parameters used in the calculations (after^{34,35}).

phonon-induced transitions and nonadiabaticity effects may then be arbitrarily small and the error is limited by the pure dephasing effect, restricting the possible gate speed-up. However, one should keep in mind that in the high frequency domain there may be additional reservoir excitations (including two-phonon processes) that are not accounted for in this model.

VI. QUANTITATIVE RESULTS FOR A MODEL PULSE SEQUENCE

In this section we calculate the errors for a STIRAP operation on a single qubit performed with specific pulse shapes. In order to get quantitative estimates and to identify the key error-inducing mechanisms in various regimes of operation we use the material parameters and QD characteristics for an InAs/GaAs system which is frequently used as the “typical” system for the proposed qubit implementations. The system parameters are collected in the Table I.

It is known that the STIRAP procedure is rather insensitive to the exact pulse shape. In order to simplify the discussion, we choose the pulse sequence

$$\Omega_{01,2}(t) = \Omega_{\text{env}}(t) \left[\frac{1 \mp \sqrt{1 - e^{-[(t \pm t_1)/\tau_0]^2}}}{2} \right]^{1/2},$$

which results in a very simple form for the time dependence of the mixing angle,

$$\sin 2\theta = e^{-\frac{1}{2} \left(\frac{t \pm t_1}{\tau_0} \right)^2}, \quad \dot{\theta} \approx \frac{1}{2\tau_0} e^{-\frac{1}{\pi} \left(\frac{t \pm t_1}{\tau_0} \right)^2}.$$

The envelope $\Omega_{\text{env}}(t)$ may be any function approximately constant around t_1 . For the numerical calculations we take

$$\Omega_{\text{env}}(t) = \Omega \frac{1 + \alpha}{1 + \alpha \cosh \left(\frac{t \pm t_1}{\tau_1} \right)},$$

with $\alpha = 10^{-4}$, $\tau_1 = 0.4\tau_0$ (Fig. 1 corresponds to this pulse choice).

For such a pulse sequence one finds explicitly from Eqs. (12,13)

$$\begin{aligned} |c_{\pm}|^2 &= 4\pi \cos^2 \frac{\vartheta}{2} \left[\frac{\sin^2 \phi}{\cos^2 \phi} \right] \sin^2[\Lambda_{\pm}(t_1)] e^{-2(\lambda_{\pm}\tau_0)^2} \\ &\leq 4\pi \cos^2 \frac{\vartheta}{2} \left[\frac{\sin^2 \phi}{\cos^2 \phi} \right] e^{-2(\lambda_{\pm}\tau_0)^2}, \end{aligned}$$

where the envelope of the oscillations has been taken as the safe bound to the error, in accordance with the discussion in Sec. III. For the purpose of analytical estimates the values of $\phi = \phi(t_1)$ and $\lambda_{\pm} = \lambda_{\pm}(t_1)$ are assumed constant. The resulting error, averaged over the initial states (11) is

$$\delta^{(\text{na})} = 2\pi \left[\sin^2 \phi e^{-2(\lambda_{-}\tau_0)^2} + \cos^2 \phi e^{-2(\lambda_{+}\tau_0)^2} \right]. \quad (38)$$

The spectral functions $s_i(\omega)$ relevant for the phonon-induced dephasing are

$$|s_1(\omega)|^2 = \frac{1}{2} \sin^2 \vartheta \frac{\pi^2}{2+\pi} \sin^2(\omega t_1) e^{-\frac{\pi}{2+\pi}(\omega\tau_0)^2} \quad (39)$$

and

$$\begin{aligned} |s_{2,3}(\omega)|^2 &= 2\pi \cos^2 \frac{\vartheta}{2} (\omega\tau_0)^2 \cos^2[\omega t_1 + \Lambda_{\mp}(t_1)] \\ &\times \left[\frac{\cos^2 \phi}{\sin^2 \phi} \right] e^{-(\omega+\lambda_{\mp})^2 \tau_0^2}. \end{aligned} \quad (40)$$

The total error is calculated as the sum of the nonadiabatic jump probability (38) and the phonon-induced contributions given by (30,31) with the spectral functions (39) and (40). The phonon spectral density corresponding to our model double-dot InAs/GaAs system is derived and discussed in the Appendix A and plotted in Fig. 2.

The resulting error as a function of the Rabi frequency Ω and detuning Δ for a fixed process duration τ_0 is shown in Fig. 3. The nontrivial interplay of the three error contributions discussed above together with the oscillating high-frequency tail of the phonon density of states $R(\omega)$ (see inset in Fig. 2b), lead to an intricate parameter dependence of the total error. There are clearly several parameter combinations for which the error becomes small. With the help of the formulas (9) one finds that the area (0a) corresponds to λ_{-} in the low-frequency region, while in (0b) λ_{+} is small and λ_{-} shifted beyond the phonon cut-off. The valleys (1), (2) ... correspond to λ_{-} positioned at one of the minima in the high-frequency tail of $R(\omega)$ and λ_{+} shifted beyond the thermal cut-off for phonon-absorption processes, i.e. $\hbar\lambda_{+} \gtrsim k_B T$. For $T = 0$ the absorption processes are not allowed at all and these areas are not separated from the (0b) region.

The detailed analysis of the error value along the (0a) valley at various temperatures (Fig. 4a) shows that at $T \neq 0$ the dependence is not monotonous. The absolute minimum always corresponds to very low Ω and Δ , for

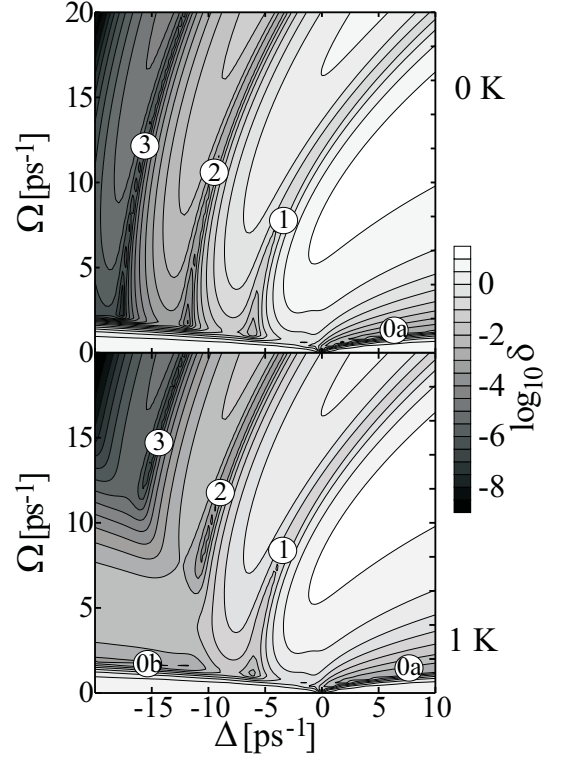


FIG. 3: The dependence of $\log_{10} \delta$ on the pulse parameters (detuning Δ and Rabi frequency Ω) at $T = 0$ and $T = 1$ K for $\tau_0 = 50$ ps. Numbers refer to the parameter regimes discussed in the text.

which both trapped states λ_{\pm} lie in the low frequency region. At high frequencies, the error values reach a plateau after passing (at $T > 0$) through a second, very shallow minimum (due to the subtle interplay of the error contributions weighted by the parameter-dependent $\sin \phi$ and $\cos \phi$ factors). In between, there is either a monotonous increase (at $T \rightarrow 0$) or a transition through a local maximum, as the λ_{+} state crosses the frequency sector with high spectral density for phonon absorption (cf. Fig 2). Fig. 4b shows the interplay between different error contributions when the Rabi frequency Ω is changed for a fixed detuning Δ . In this range of parameters, for the specific system under study, the pure dephasing contribution turns out to be small compared to the errors related to real phonon-induced transitions and to nonadiabatic jumps which create a trade-off situation with one or two well-defined parameter sets corresponding to the minimal errors.

The above results show that for a fixed pulse duration τ_0 the error values are bounded from below, precluding a perfect operation for any parameter values. However, due to the super-ohmic behavior of all the contributions to the phonon spectral density (at low frequencies), the total error is decreased when the process time grows and the trapped level splittings decrease. The minimum er-

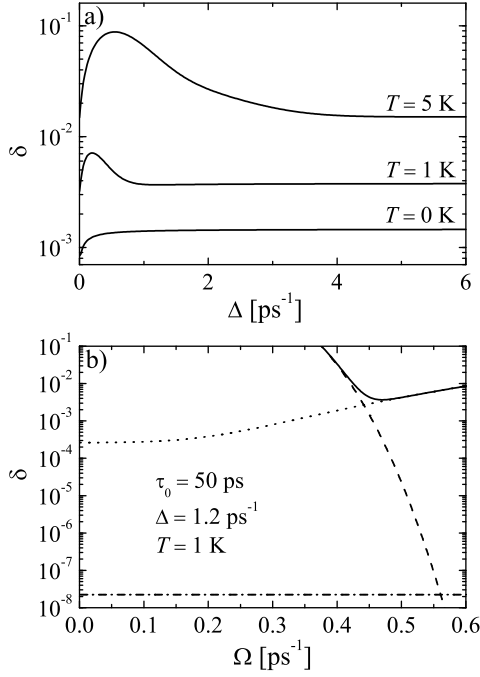


FIG. 4: (a) The dependence of the error for growing detuning with $\lambda_- = \text{const}$, along the (0a) minimum in Fig. 3. (b) The total error (solid) and the individual contributions: nonadiabatic jumps (dashed), phonon-assisted real transitions (dotted) and pure dephasing (dash-dotted) for a section of the parameter space.

ror achievable for different process durations at various temperatures is plotted in Fig. 5a,b and the corresponding laser beam parameters are shown in Fig. 5c,d. Both the values at the global minimum (Fig. 5a,c) and at the shallow local minimum (Fig. 5b,d) are shown. In order to allow for any subtle interplay of parameters, for each τ_0 the full minimization with respect to both Δ and Ω was performed. As expected, the error decreases for longer pulse durations, but the decrease is only polynomial ($\delta \sim 1/\tau_0$ at higher temperatures and $\tau_0 \gtrsim 10$ ps). Therefore, rather long pulse durations are necessary to reduce the error considerably. Moreover, the optimization is obtained for rather unusually small parameter values (Fig. 5b) and is very sensitive to their precision. Still another restriction is that in this low-frequency regime the optimum is searched against the nonadiabatic jump error and is reached for $\tau_0 \lambda_{\pm} \gtrsim 1$. As soon as τ_0 becomes comparable to the trion radiative lifetime (~ 1 ns), the optimal value of λ_{\pm} falls within the broadening of the $|3\rangle$ state, disabling the adiabatic passage.

The parameter dependence of the error in the (0b) area is in a way analogous. Here, however, it is $|\lambda_-|$ that must be shifted far beyond the positive frequency cut-off. Even at zero temperature, the positive-frequency part of

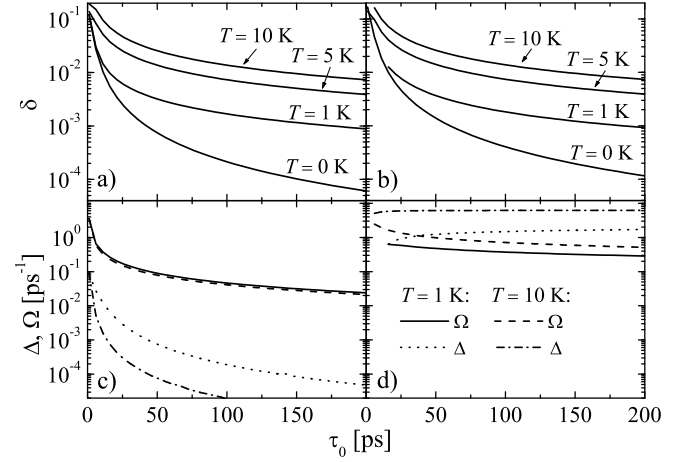


FIG. 5: (a,b) The minimal achievable error as a function of the process duration corresponding to the optimal pulse parameters with both λ_{\pm} in the low-frequency area (a) and with λ_+ in the high frequency area (b) (for $T = 0$ the plateau value for $\Delta \rightarrow \infty$ is shown). (c,d) The optimal pulse parameters (detuning and Rabi frequency) realizing the minimal error for these two configurations. The legend in (d) applies to both (c,d).

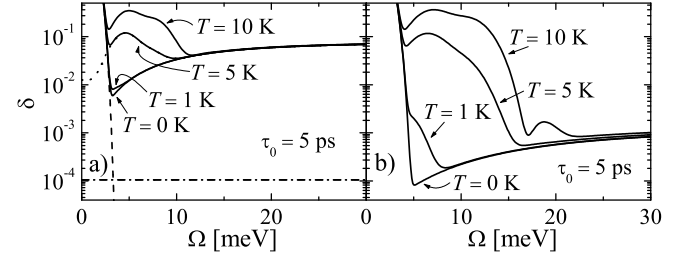


FIG. 6: The error as a function of Ω for $\lambda_- = \text{const}$, along the 1 (a) and 2 (b) areas in Fig. 3. In (a) the individual contributions to the error at $T = 5$ K are also shown: nonadiabatic jumps (dashed), phonon-assisted real transitions (dotted) and pure dephasing (dash-dotted).

the spectral density extends to relatively high frequencies (with oscillations manifesting themselves as local minima in Fig. 3b). Therefore, this parameter regime is always less favorable than the previous one.

In view of the limited possibility of fidelity optimization in the low-frequency region for reasonable process durations, it is interesting to study the high-frequency parameter range. In contrast to the previous case, the values of Ω and Δ may now seem unusually high, but the results of Fig. 3 show that by increasing the splitting between the trapped state energies the error may in principle be reduced to arbitrarily low values.

The Figure 6 shows the error along the (1) and (2) area (Fig. 3) for fixed pulse duration at various temper-

atures, as well as the contributions to the error in one case. The trapped states are now split by several meV, so that the nonadiabatic error is negligible (except for sub-picosecond pulses). However, the speeding-up of the dynamics is limited by the pure-dephasing contribution. On the other hand, extending the pulse duration is unfavorable due to the phonon-assisted transitions. The interplay of these two contributions for a given pulse duration, temperature and λ_- yields a series of minima, corresponding to λ_+ traveling across the oscillations of $R(\omega)$, as shown in Fig. 6. Note that at low temperatures only one minimum exists, belonging actually to the (0b) parameter area, but at higher temperatures the absolute minimum shifts to the high-frequency region.

The minimum value reached depends on the pulse duration, with a certain optimal trade-off which depends, however, on the chosen value of λ_- and decreases substantially for subsequent minima of the spectral density. The resulting minimum value, obtained by numerical minimization with respect to Ω and Δ for a range of pulse durations, is shown in Fig. 7a,b. The individual contributions shown in Fig. 7a show that pure dephasing indeed limits the fidelity for short pulses but in the optimal duration range the non-monotonous τ_0 -dependence of the error is determined exclusively by the phonon-assisted transition contribution. This astonishing effect is in fact due to the relatively narrow minimum of $R(\omega)$ in which $|\lambda_-|$ is placed. For short pulses, $s_3(\omega)$ becomes broad (pure dephasing broadening of the λ_- level), increasing the overlap with $R(\omega)$. For large τ_0 , the linear increase of δ due to long process duration becomes dominating, leading to a minimum at a certain point.

VII. CONCLUSIONS

We have studied the fidelity of the coherent operation on a QD spin qubit rotated by a stimulated Raman adiabatic passage to a neighboring dot and back. We have shown that, in addition to the usual limitation of the speed of an adiabatic process, the presence of the phonon reservoir imposes two further restrictions: The transfer must be slow in order to minimize the pure dephasing effect but it should not take too long in order to avoid transitions between the trapped carrier-light states. The general formalism was applied to an InAs/GaAs self-assembled system of typical size. It turns out that for most values of pulse parameters (intensities and detuning) in meV range the error is high enough to totally prevent the coherent operation. However, there are also narrow parameter areas where the fidelity is considerably higher.

The super-ohmic characteristics of the spectral density associated with the phonon reservoir admits minimization of the total error by increasing the duration of the process while simultaneously decreasing the trapped level energies. However, the pulse durations necessary for a considerable reduction of the error in this low-frequency

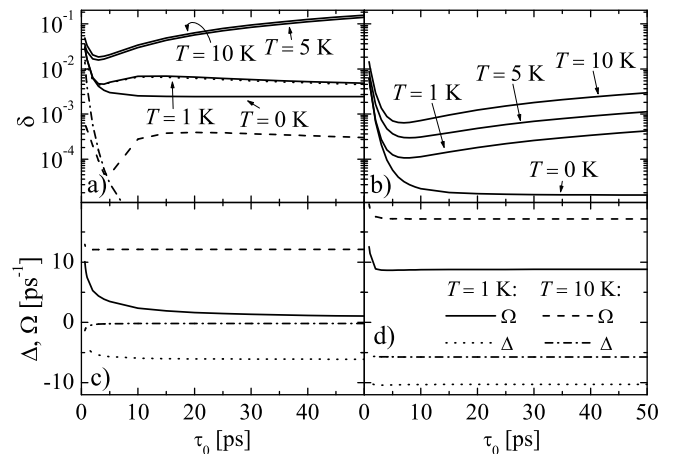


FIG. 7: (a,b) The minimal achievable error as a function of the process duration corresponding to the optimal pulse parameters with both λ_{\pm} in the high-frequency parameter areas 1 (a) and 2 (b) and the optimal pulse parameters (detuning and Rabi frequency) realizing the minimal error for these two configurations (c,d). In (a) the contributions to the error at $T = 1$ K are shown: nonadiabatic jumps (dashed), phonon-assisted real transitions (dotted) and pure dephasing (dash-dotted).

regime are of order of hundreds of picoseconds which leads to nanosecond overall gate durations (full sequence of two pairs of pulses). Moreover, the resulting trapped state energies become extremely small, approaching the typical lifetime broadening of the trion state used for the Raman coupling.

It is found that the qubit operation may be performed with much higher fidelity if the trapped states are pushed beyond the cut-off of the effectively coupled phonon modes. An additional advantage comes from the oscillatory structure of the phonon spectral density for a double-dot system. In this way the error at $T = 0$ may be reduced to the value of $\sim 10^{-3}$ and well below 10^{-4} for the trapped state energy splitting of 4 meV and 8 meV, respectively (for the system geometry used). The latter values lie in the spectral region where the acoustic phonon effects dominate the decoherence, well below any spectral features (LO phonons, higher exciton states) not included in the discussion. It is remarkable that such low error values are achieved with pulse durations of the order of 10 ps which, compared to the electron spin decoherence time of tens of μ s, opens a broad time window for a large number of gating operations.

These optimistic conclusions are somewhat limited by the strong temperature dependence of phonon occupations, especially in the low-frequency regime, leading to a fast increase of the error at non-zero temperatures. Indeed, in some cases the minimal error may grow even by an order of magnitude as soon as the temperature reaches 1 K.

The strong dependence of the phonon-related error

on the material parameters and system geometry opens some possibility of system engineering and optimization. For example, the high-frequency asymptotics of the phonon spectral density is governed by the QD height: higher dots assure a faster decay. On the other hand, in the low-frequency sector the phonon spectral density scales with the square of the inter-dot distance, favoring rather flat structures. Also increasing the lateral size reduces the phonon coupling but, at the same time, lowers the excited states restricting the high-frequency range of operation. This shows that finding the optimum may be nontrivial and may depend on the frequency sector chosen for the qubit operation. It should be noted that the high-frequency spectral density is dominated by the deformation potential coupling which is present in any semiconductor system but in the low-frequency domain the piezoelectric effects dominate. This might suggest using non-piezoelectric materials.

Let us note also that the single-qubit error calculated in this paper gives also an estimate of the two-qubit operation if the latter is performed using dipole coupling between the auxiliary states in the STIRAP scheme.¹⁸

Acknowledgments

This work was supported by the Polish Ministry of Scientific Research and Information Technology under the (solicited) Grant No. PBZ-MIN-008/P03/2003 and by the Polish KBN under Grant No. PB 2 P03B 085 25. P.M. is grateful to the Humboldt Foundation for support.

APPENDIX A: PHONON COUPLINGS AND SPECTRAL DENSITIES

In this appendix we derive the spectral density of the phonon reservoir $R_{22}(\omega)$ and study its properties for low and high frequencies.

The phonon coupling constants $F_{22}(\mathbf{k}) = f_{22}(\mathbf{k}) - f_{00}(\mathbf{k})$ have the same structure as the original constants [Eq. (4a,b)] with the formfactor replaced by $\mathcal{F}(\mathbf{k}) = \mathcal{F}_{22}(\mathbf{k}) - \mathcal{F}_{00}(\mathbf{k})$. Let $\mathcal{F}_{L,S}(\mathbf{k})$ denote the formfactors, calculated according to Eq. (5), for the ground-state electronic wave-function in the large (L) and small (S) dot. Assuming that the dots are stacked along the z axis at the distance D , one has

$$\mathcal{F}(\mathbf{k}) = e^{i\frac{Dk_z}{2}} \mathcal{F}_S(\mathbf{k}) - e^{-i\frac{Dk_z}{2}} \mathcal{F}_L(\mathbf{k}).$$

The long-wavelength properties of the coupling constants do not depend on the wave-function geometry. Indeed, $\mathcal{F}_{S,L}(\mathbf{k}) = 1 + O(k^2)$ and $\mathcal{F}(\mathbf{k}) = iDk_z + O(k^3)$.

The coupling constants for arbitrary \mathbf{k} depend obviously on the specific form of the wave-functions. For simplicity, we assume Gaussian wave-functions,

$$\Psi_{L,S}(\mathbf{r}) = N \exp \left[-\frac{1}{2} \left(\frac{\mathbf{r}_\perp}{l_{\perp,L,S}} \right)^2 - \frac{1}{2} \left(\frac{z}{l_{z,L,S}} \right)^2 \right].$$

Then

$$\mathcal{F}_{S,L}(\mathbf{k}) = e^{-\left(\frac{k_\perp l_{\perp,L,S}}{2}\right)^2} e^{-\left(\frac{k_z l_{z,L,S}}{2}\right)^2}.$$

Allowing for a small difference between the dot sizes we write $l_{\perp,L,S}^2 = l_\perp^2 \pm \frac{1}{2}\Delta(l_\perp^2)$, $l_{z,L,S}^2 = l_z^2 \pm \frac{1}{2}\Delta(l_z^2)$, so that

$$\begin{aligned} \mathcal{F}(\mathbf{k}) &\approx e^{-\left(\frac{k_\perp l_\perp}{2}\right)^2} e^{-\left(\frac{k_z l_z}{2}\right)^2} \\ &\times \left[2i \sin \frac{Dk_z}{2} + \frac{k_\perp^2 \Delta(l_\perp^2) + k_z^2 \Delta(l_z^2)}{4} \cos \frac{Dk_z}{2} \right]. \end{aligned}$$

Hence, the size difference brings only a small correction and will be neglected.

Assuming isotropic phonon dispersions, the spectral density $R(\omega) = R_{22,22}(\omega)$ (24) may be written as

$$\begin{aligned} R(\omega) &= \frac{V}{(2\pi)^3} \sum_s \int dk k^2 \\ &\times [(n_k + 1)\delta(\omega - \omega_k) + n_k \delta(\omega + \omega_k)] \\ &\times \frac{1}{\hbar^2} \int \cos \theta d\theta \int d\varphi |F_{22}^{(s)}(\mathbf{k})|^2. \end{aligned}$$

The LA phonons are coupled both via piezoelectric and deformation potential interaction. However, due to different inversion symmetry the mixed terms vanish upon angle integration and the two terms contribute independently.

The deformation potential term is

$$R^{(\text{DP})}(\omega) = R_0^{(\text{DP})} \omega^5 [n_B(\omega) + 1] f^{(\text{DP})}(\omega),$$

where

$$R_0^{(\text{DP})} = \frac{1}{3(2\pi)^2} \frac{D^2 \sigma_e^2}{\hbar \rho c_l^7}$$

and the function $f^{(\text{DP})}(\omega)$ is defined as

$$\begin{aligned} f^{(\text{DP})}(\omega) &= \frac{3}{2} \int_{-\pi/2}^{\pi/2} d\theta \cos \theta \frac{4 \sin^2 \left(\frac{D\omega}{2c_l} \sin \theta \right)}{\left(\frac{D\omega}{2c_l} \right)^2} \\ &\times \exp \left[-\frac{1}{2} \left(\frac{\omega l_\perp}{c_l} \right)^2 \left(\cos^2 \theta + \frac{l_z^2}{l_\perp^2} \sin^2 \theta \right) \right], \end{aligned} \quad (\text{A1})$$

so that $f^{(\text{DP})}(\omega) \rightarrow 1$ as $\omega \rightarrow 0$.

For the piezoelectric contributions we choose the phonon polarizations

$$\begin{aligned} \hat{e}_{1,\mathbf{k}} &\equiv \hat{\mathbf{k}} = (\cos \theta \cos \phi, \cos \theta \sin \phi, \sin \theta), \\ \hat{e}_{t1,\mathbf{k}} &= (-\sin \phi, \cos \phi, 0), \\ \hat{e}_{t2,\mathbf{k}} &= (\sin \theta \cos \phi, \sin \theta \sin \phi, -\cos \theta); \end{aligned}$$

then the functions M_s are

$$\begin{aligned} M_1 &= \frac{3}{2} \sin 2\theta \cos \theta \sin 2\phi, \\ M_{t1} &= \sin 2\theta \cos 2\phi, \\ M_{t2} &= (3 \sin^2 \theta - 1) \cos \theta \sin 2\phi. \end{aligned}$$

The corresponding terms in the spectral density are

$$R^{(P)}(\omega) = \sum_s R_0^{(P,s)} \omega^3 [n_B(\omega) + 1] f^{(P,s)}(\omega),$$

where

$$R_0^{(P,s)} = \frac{1}{2\hbar\rho(2\pi)^3 c_s^5} \mu_s \left(\frac{edD}{\epsilon_0\epsilon_1} \right)^2,$$

$$f^{(P,s)}(\omega) = \frac{1}{\mu_s} \int_{-\pi/2}^{\pi/2} d\theta \cos\theta M_s^2(\theta) \frac{4 \sin^2 \left(\frac{D\omega}{2c_1} \sin\theta \right)}{\left(\frac{D\omega}{2c_1} \right)^2}$$

$$\times e^{-\frac{1}{2} \left(\frac{\omega l_1}{c_1} \right)^2 \left[\cos^2\theta + \frac{l_z^2}{l_1^2} \sin^2\theta \right]},$$

$f^{(P,s)}(\omega) \rightarrow 1$ as $\omega \rightarrow 0$, and

$$M_s^2(\theta) = \int d\varphi M_s^2(\theta, \varphi), \quad \mu_s = \int d\theta \cos\theta M_s^2(\theta).$$

Thus, the low-frequency behavior of the individual contributions to the spectral density is $\sim \omega^3$ and $\sim \omega^5$ for the piezoelectric and deformation potential coupling, respectively.

The behavior in the high frequency limit is determined by the coupling to phonons with wavevectors in the strongest confinement direction, i.e. along the z axis. The piezoelectric coupling in this direction is suppressed by the geometrical factors M_s and the corresponding contributions to the spectral function decrease rapidly. Moreover, the frequencies of TA phonons are relatively low and the piezoelectric coupling to LA phonons is much weaker. The frequencies of LA phonons reach much higher values, e.g. over 20 meV for GaAs, and their dispersion remains approximately isotropic and linear up to several meV.³⁵ Expanding the integral into an asymptotic series one finds an upper estimate for (A1),

$$f^{(DP)}(\omega) \lesssim \frac{12c_1^4}{D^2(l_1^2 - l_z^2)} \frac{1}{\omega^4} e^{-\frac{1}{2} \left(\frac{l_z \omega}{c_1} \right)^2}.$$

In vicinity of the points $\omega_n = 4n\pi c_1/D$, the following lower bound approximately holds

$$f^{(DP)}(\omega) \gtrsim \frac{3c_1^6}{(l_1^2 - l_z^2)^3} \frac{1}{\omega^6} e^{-\frac{1}{2} \left(\frac{l_z \omega}{c_1} \right)^2},$$

(see Fig. 2b) The oscillatory behavior of the spectral density for large frequencies follows from the fact that

the predominant contribution in this sector comes from phonons along the strongest confinement direction, leading to a pronounced destructive interference of interaction amplitudes in the double-dot structure aligned along this direction.

APPENDIX B: TRANSITIONS BETWEEN THE TRAPPED STATES: FERMI GOLDEN RULE

Inserting the definition (34b) into the Eq. (36) and performing the frequency integration (for $\lambda_{\pm}, \phi \approx \text{const}$) we get

$$\delta_{\mp}^{(\text{tr})} \approx \cos^2 \frac{\vartheta}{2} \frac{\pi}{2} R(-\lambda_{\mp}) \left[\frac{\cos^2 \phi}{\sin^2 \phi} \right] \int dt \sin^2 2\theta(t). \quad (\text{B1})$$

Let us now consider the probability of phonon absorption or emission leading to a transition from the state $|a_0\rangle$ to $|a_{\pm}\rangle$. The duration of a single absorption or emission process is of order of inverse phonon frequency (i.e. trapped level spacing). Hence, in view of the adiabaticity condition (15) this process is fast compared to the characteristic time scale of the system evolution. Therefore, it is reasonable to calculate the Fermi Golden Rule (FGR) probability for absorption or emission at fixed values of system parameters and include the time-dependence related to the STIRAP passage only at the level of the rate equations. Assuming the initial state (11), taking the matrix element of the phonon coupling Hamiltonian (6) between the trapped states (8a-c) and applying the FGR in the standard form one finds for the transition probability

$$w_{\mp}(t) = \frac{2\pi}{\hbar} \frac{1}{4} \cos^2 \frac{\vartheta}{2} \left[\frac{\cos^2 \phi}{\sin^2 \phi} \right] \sin^2 2\theta(t) \sum_{\mathbf{k}} |F(\mathbf{k})|^2$$

$$\times [\delta(\hbar\lambda_{\mp} - \hbar\omega_{\mathbf{k}}) n_{\mathbf{k}} + \delta(\hbar\lambda_{\mp} + \hbar\omega_{\mathbf{k}}) (n_{\mathbf{k}} + 1)]$$

$$= \frac{\pi}{2} \cos^2 \frac{\vartheta}{2} \left[\frac{\cos^2 \phi}{\sin^2 \phi} \right] \sin^2 2\theta(t) R(-\lambda_{\mp}).$$

Solving the rate equation for the jump probability with the above time-dependent rate $w(t)$ we find the error probability for the whole process duration

$$\delta_{\mp}^{(\text{tr})} = 1 - \exp \left[- \int_{-\infty}^{\infty} w_{\mp}(t) dt \right]. \quad (\text{B2})$$

For small error values this reduces to (B1). However, it gives also an estimate for the error beyond the applicability of the perturbative treatment.

* Electronic address: Pawel.Machnikowski@pwr.wroc.pl

¹ *The Physics of Quantum Information*, edited by D. Bouwmeester, A. Eckert, and A. Zeilinger (Springer-Verlag, Berlin Heidelberg, 2000).

² L. Jacak, P. Hawrylak, and A. Wojs, *Quantum Dots* (Springer Verlag, Berlin, 1998).

³ R. Hanson, B. Witkamp, L. M. K. Vandersypen, L. H. Willems van Beveren, J. M. Elzerman, and L. P. Kouwen-

- hoven, Phys. Rev. Lett. **91**, 196802 (2003).
- ⁴ D. Loss and D. P. DiVincenzo, Phys. Rev. A **57**, 120 (1998).
 - ⁵ T. H. Stievater, X. Li, D. G. Steel, D. Gammon, D. S. Katzer, D. Park, C. Piermarocchi, and L. J. Sham, Phys. Rev. Lett. **87**, 133603 (2001).
 - ⁶ H. Kamada, H. Gotoh, J. Temmyo, T. Takagahara, and H. Ando, Phys. Rev. Lett. **87**, 246401 (2001).
 - ⁷ H. Htoon, T. Takagahara, D. Kulik, O. Baklenov, A. L. Holmes Jr., and C. K. Shih, Phys. Rev. Lett. **88**, 087401 (2002).
 - ⁸ A. Zrenner, E. Beham, S. Stuffer, F. Findeis, M. Bichler, and G. Abstreiter, Nature **418**, 612 (2002).
 - ⁹ P. Borri, W. Langbein, S. Schneider, U. Woggon, R. L. Sellin, D. Ouyang, and D. Bimberg, Phys. Rev. B **66**, 081306 (2002).
 - ¹⁰ X. Li, Y. W. D. Steel, D. Gammon, T. Stievater, D. Katzer, D. Park, C. Piermarocchi, and L. Sham, Science **301**, 809 (2003).
 - ¹¹ E. Biolatti, R. C. Iotti, P. Zanardi, and F. Rossi, Phys. Rev. Lett. **85**, 5647 (2000).
 - ¹² P. Borri, W. Langbein, S. Schneider, U. Woggon, R. L. Sellin, D. Ouyang, and D. Bimberg, Phys. Rev. Lett. **87**, 157401 (2001).
 - ¹³ M. Bayer and A. Forchel, Phys. Rev. B **65**, 041308 (2002).
 - ¹⁴ E. Pazy, E. Biolatti, T. Calarco, I. D'Amico, P. Zanardi, F. Rossi, and P. Zoller, Europhys. Lett. **62**, 175 (2003).
 - ¹⁵ T. Calarco, A. Datta, P. Fedichev, E. Pazy, and P. Zoller, Phys. Rev. A **68**, 12310 (2003).
 - ¹⁶ A. Imamoglu, D. D. Awschalom, G. Burkard, D. P. DiVincenzo, D. Loss, M. Sherwin, and A. Small, Phys. Rev. Lett. **83**, 4204 (1999).
 - ¹⁷ M. Feng, I. D'Amico, P. Zanardi, and F. Rossi, Phys. Rev. B **67**, 014306 (2003).
 - ¹⁸ F. Troiani, E. Molinari, and U. Hohenester, Phys. Rev. Lett. **90**, 206802 (2003).
 - ¹⁹ Z. Kis and F. Renzoni, Phys. Rev. A **65**, 032318 (2002).
 - ²⁰ U. Hohenester, F. Troiani, E. Molinari, G. Panzarini, and C. Macchiavello, Appl. Phys. Lett. **77**, 1864 (2000).
 - ²¹ Pochung Chen, C. Piermarocchi, L. J. Sham, D. Gammon, and D. G. Steel, Phys. Rev. B **69**, 075320 (2004).
 - ²² K. Bergmann, H. Teuer, and B. W. Shore, Rev. Mod. Phys. **70**, 1003 (1998).
 - ²³ H.-P. Breuer and F. Petruccione, *The Theory of Open Quantum Systems* (Oxford University Press, Oxford, 2002).
 - ²⁴ B. Krummheuer, V. M. Axt, and T. Kuhn, Phys. Rev. B **65**, 195313 (2002).
 - ²⁵ A. Vagov, V. M. Axt, and T. Kuhn, Phys. Rev. B **66**, 165312 (2002).
 - ²⁶ L. Jacak, P. Machnikowski, J. Krasnyj, and P. Zoller, Eur. Phys. J. D **22**, 319 (2003).
 - ²⁷ A. Vagov, V. M. Axt, and T. Kuhn, Phys. Rev. B **67**, 115338 (2003).
 - ²⁸ R. Alicki, M. Horodecki, P. Horodecki, R. Horodecki, L. Jacak, and P. Machnikowski, quant-ph/0302058 (unpublished).
 - ²⁹ G. D. Mahan, *Many-Particle Physics* (Kluwer, New York, 2000).
 - ³⁰ G. D. Mahan, in *Polarons in Ionic Crystals and Polar Semiconductors*, edited by J. T. Devreese (North-Holland, Amsterdam, 1972).
 - ³¹ A. Messiah, *Quantum Mechanics* (North-Holland, Amsterdam, 1966).
 - ³² R. Alicki, M. Horodecki, P. Horodecki, and R. Horodecki, Phys. Rev. A **65**, 062101 (2002), quant-ph/0105115.
 - ³³ C. Cohen-Tannoudji, J. Dupont-Roc, and G. Grynberg, *Atom-Phonon Interactions* (Wiley-Interscience, New York, 1998).
 - ³⁴ S. Adachi, J. Appl. Phys. **58**, R1 (1985).
 - ³⁵ D. Strauch and B. Dörner, J. Phys: Cond. Matt. **2**, 1457 (1990).